Oligomeric State of Human Erythrocyte Band 3 Measured by Fluorescence Resonance Energy Homotransfer

Scott M. Blackman, David W. Piston, and Albert H. Beth
Department of Molecular Physiology and Biophysics, Vanderbilt University, Nashville, Tennessee 37232-0615 USA

ABSTRACT The oligomeric state of the erythrocyte anion exchange protein, band 3, has been assayed by resonance energy homotransfer. Homotransfer between oligomeric subunits, labeled with eosin-5-maleimide at Lys^{430} in the transmembrane domain, has been demonstrated by steady-state and time-resolved fluorescence spectroscopy, and is readily observed by its depolarization of the eosin fluorescence. Polarized fluorescence measurements of HPLC-purified band 3 oligomers indicate that eosin homotransfer increases progressively with increasing species size. This shows that homotransfer also occurs between labeled band 3 dimers as well as within the dimers, making fluorescence anisotropy measurements sensitive to band 3 self-association. Treatment of ghost membranes with either Zn^{2+} or melittin, agents that cluster band 3, significantly decreases the anisotropy as a result of the increased homotransfer within the band 3 clusters. By comparison with the anisotropy of species of known oligomeric state, the anisotropy of erythrocyte ghost membranes at 37°C is consistent with dimeric and/or tetrameric band 3, and does not require postulation of a fraction of large clusters. Proteolytic removal of the cytoplasmic domain of band 3, which significantly increases the rotational mobility of the transmembrane domain, does not affect its oligomeric state, as reported by eosin homotransfer. These results support a model in which interaction with the membrane skeleton restricts the mobility of band 3 without significantly altering its self-association state.

INTRODUCTION

The erythrocyte anion exchange protein, band 3 (also known as AE1), provides a major mechanical linkage between the membrane skeleton and the lipid bilayer that is required for maintaining the proper shape and flexibility of erythrocytes (reviewed in Palek and Lambert, 1990; Wang, 1994; see also Peters et al., 1996; Southgate et al., 1996). Like many other integral membrane proteins, band 3 forms oligomers. A large body of evidence, including chemical cross-linking data (Steck, 1972; Jennings and Nicknish, 1985; Staros and Kakkad, 1983) and a low-resolution electron diffraction structure (Wang et al., 1993, 1994), indicates that the minimum structural unit of band 3 is the dimer. Other studies have suggested the existence of higher order oligomers ranging from tetramers (Weinstein et al., 1980; Benz et al., 1984; Casey and Reithmeier, 1991) to much larger clusters of band 3 (Cherry et al., 1976; Rodgers and Glaser, 1993). Formation of tetramers has been implicated in binding to the erythrocyte cytoskeleton via ankyrin (Thevenin and Low, 1990; Casey and Reithmeier, 1991; Mulzer et al., 1991; Pinder et al., 1995; Michaely and Bennett, 1995; Che et al., 1997; Yi et al., 1997).

Determining the in situ oligomeric state and interactions of integral membrane proteins is important for understanding their structural and functional roles in cell physiology, as is apparent from studies on many systems, including calcium ATPase (Shi et al., 1996) and epidermal growth factor receptor (Zidovetzki et al., 1991). One means of assessing the distribution of integral membrane protein oligomeric states in situ is provided by spectroscopic measurements of protein rotational diffusion. The uniaxial rotational diffusion model (Saffman and Delbrück, 1975; Jähnig, 1986) predicts that the rotational dynamics of integral membrane proteins are strongly dependent on the intramembrane radius and thus the oligomeric state of the mobile unit. Therefore, the determination of the rotational diffusion coefficients and the fractional amplitudes of each distinct rotational species can, in theory, provide a measure of oligomeric states. Band 3 rotational dynamics on the microsecond to millisecond time scale have been studied by electron paramagnetic resonance (EPR) (Hustedt and Beth, 1995, 1996) and optical (e.g., Cherry et al., 1976; Tsuji et al., 1988; Matayoshi and Jovin, 1991; McPherson et al., 1993; Corbett and Golan, 1993; Blackman et al., 1996) techniques, with apparently conflicting results. Optical studies detect a complex set of anisotropy decay times ranging from tens of microseconds to several milliseconds (e.g., Matayoshi and Jovin, 1991). These results have been interpreted phenomenologically to indicate a heterogeneous mixture of oligomers ranging from highly mobile dimers to essentially immobilized clusters. In contrast, saturation transfer EPR (ST-EPR) studies of band 3 detect a single uniaxial rotational motion of large amplitude, which is consistent with rotational diffusion of band 3 dimers or tetramers; no significant fraction of slowly rotating or immobilized band 3 is detected (Hustedt and Beth, 1995, 1996). The discrepancy likely arises because of the sensitivity of rotational dynamics to phenomena other than oligomerization, such as dynamics of the lipid bilayer (e.g., Van der Meer, 1993), binding to cytoskeletal proteins, or rotational motions not included in the uniaxial rotational

Received for publication 3 February 1998 and in final form 4 May 1998.
Address reprint requests to Dr. Albert H. Beth, Department of Molecular Physiology and Biophysics, 702 Light Hall, Vanderbilt University, Nashville, Tennessee, 37232-0615. Tel.: 615-322-4235; Fax: 615-322-7236; E-mail: beth@lhmrba.hh.vanderbilt.edu.

0006-3495/98/08/1117/14 $2.00

diffusion model (discussed in Hustedt and Beth, 1995). A second result reported by optical rotational diffusion measurements is that after proteolytic cleavage of band 3 to separate its integral membrane domain from its cytoplasmic cytoskeleton-binding domain, band 3 rotational mobility is significantly increased (e.g., Nigg and Cherry, 1980). Previous measurements have not been able to distinguish between two proposed mechanisms for this mobility increase: 1) release of a population of band 3 whose rotational diffusion is limited by interaction with the cytoskeleton (Nigg and Cherry, 1980), and 2) disruption of clusters of band 3, which are induced to form by the cytoskeleton (Nigg and Cherry, 1980; Clague et al., 1989; Wyatt and Cherry, 1992).

The above discussion highlights some of the problems with assigning molecular species based solely upon rotational diffusion measurements. For band 3, a complementary means of observing oligomeric states in situ would be valuable in addressing the questions raised by the rotational dynamics studies. Size-exclusion high-performance liquid chromatography (HPLC) (Casey and Reithmeier, 1991) and analytical ultracentrifugation (Schuck et al., 1995) have proved very useful in defining the sizes and proportions of band 3 oligomers in detergent solution, but cannot be used on band 3 in situ. In intact membranes or in detergent solution, the dimensions of band 3 oligomers can theoretically be measured by resonance energy heterotransfer (occurring between distinct donor and acceptor species) or homotransfer (occurring between labels of the same species). Indeed, resonance energy homotransfer, occurring between adjacent fluorescein-labeled cytoplasmic domains of band 3, has been used to demonstrate that band 3 in erythrocyte-derived lipid vesicles is not predominantly monomeric (Dissing et al., 1979). Formation of band 3 oligomers larger than dimers was not investigated in any detail in that report. In the present studies, the extracellular face of the membrane domain of band 3 was labeled at Lys^{430} with eosin-5-maleimide (EMA) (Nigg and Cherry, 1979a,b; Cobb and Beth, 1990), a commonly used fluorescent and phosphorescent affinity label for band 3 (e.g., Nigg and Cherry, 1980; Tsuji et al., 1988; Matayoshi and Jovin, 1991; McPherson et al., 1993; Corbett and Golan, 1993; Blackman et al., 1996).

Resonance energy homotransfer has now been shown to occur in EMA-labeled band 3 by measuring the excitation wavelength and stoichiometry dependence of the fluorescence anisotropy and lifetime. Calculations of its effective distance range (R_0) suggest that homotransfer can occur between the labeled integral membrane domains of band 3 monomers in a dimer (intradimer homotransfer) and between dimers in larger oligomers (interdimer homotransfer). This hypothesis has been confirmed by studies on detergent-solubilized oligomers purified by size-exclusion HPLC, and on experimentally created band 3 clusters in situ, both of which demonstrate that steady-state fluorescence anisotropy measurements are sensitive to the oligomeric state of band 3. This provides a spectroscopic method that does not rely on measuring rotational dynamics for assaying the further self-association of band 3 dimers in the erythrocyte ghost membrane. Homotransfer results from ghost membranes at 37°C can be interpreted most simply as arising from dimeric and tetrameric band 3 alone, without requiring an additional clustered fraction. This suggests that interpretations of rotational diffusion data in terms of a very large fraction of clustered band 3 (e.g., Wyatt and Cherry, 1992) should be questioned. In addition, proteolytic separation of the membrane and cytoplasmic domains of band 3 has no effect on its self-association state at 37°C, as reported by EMA homotransfer. This clearly indicates that the increase in rotational mobility after proteolytic cleavage (Nigg and Cherry, 1980; Matayoshi and Jovin, 1991; Blackman et al., 1996) is not due to the disruption of band 3 clusters, and suggests that, instead, trypsin proteolysis releases a population of band 3 whose amplitude of rotational diffusion is limited by its interaction with the cytoskeleton. Portions of this work have been published previously in abstracts (Blackman et al., 1997, 1998).

MATERIALS AND METHODS

Preparation of erythrocyte ghost samples

EMA-labeled erythrocyte ghost membranes were prepared as described previously (Blackman et al., 1996). To achieve maximum EMA labeling, 1 volume of EMA solution (0.5 mg/ml in 113 mM sodium citrate, pH 7.4) was added to 5 volumes of washed erythrocytes at 50% hematocrit (a 10- to 15-fold molar excess; Nigg and Cherry, 1979b; Cobb and Beth, 1990). For labeling at lower EMA stoichiometries, the concentration of EMA in the stock solution was decreased. Unsealed erythrocyte ghosts were prepared by hypotonic lysis in ice-cold 5P7.4 (5 mM sodium phosphate, pH 7.4) with repeated washing, yielding white (or pink for EMA-labeled ghosts) pellets of 2–2.5 mg/ml total protein concentration. Mild proteolysis with L-1-tosylamide-2-phenylethyl chloromethyl ketone (TPCK)-treated trypsin (Sigma, St. Louis, MO) was performed for 30 min on ice as described previously (Blackman et al., 1996), except that 3 μg/ml was sufficient to produce >90% cleavage, as shown by sodium dodecyl sulfate-polyacrylamide gel electrophoresis (SDS-PAGE) (Laemmli, 1970). Cytoskeleton-depleted (stripped) ghosts were made using 2 mM EDTA, pH 12, as described by Casey et al. (1989), except that the resulting ghosts were washed with 5P7.4 containing 20 μg/ml phenylmethylsulfonyl fluoride (PMSF) to inhibit proteolysis of the cytoplasmic domain. For melittin treatment, a stock solution of 1 mg/ml melittin (Sigma) in 5P7.4 was used in studies on ghost membranes diluted 100–200 fold in 5P7.4. For treatment with Zn^{2+}, a stock solution of ~5 mM $ZnCl_2$ in HEPES buffer (10 mM HEPES, pH 7.4) was added to erythrocyte ghost membranes that had been washed in HEPES buffer and diluted 100–200-fold.

Solubilized ghost samples were prepared by adding 1 volume of a 10% $C_{12}E_8$ (polyoxyethylene 8 lauryl ether; Sigma) solution (in 5P7.4) to 9 volumes of ghosts at 2–2.5 mg/ml protein concentration. Some samples were solubilized by dilution into 5 volumes of 1% $C_{12}E_8$ (Casey et al., 1989), yielding identical HPLC chromatographs and anisotropy values. After incubating for at least 15 min on ice, each sample was centrifuged at 4°C in a tabletop microcentrifuge (15 min, 13,000 rpm), and the supernatant was collected. Control membranes had a small pellet that was enriched for bands 1 and 2 relative to band 3. Trypsin-treated membranes had no pellet, and EDTA-stripped membranes had only a very tiny pellet that did not contain band 3, as shown by SDS-PAGE.

To measure band 3 concentration in EMA-labeled samples, the total protein concentration was determined in duplicate by BCA (bicinchoninic acid) assay (Sigma). The ratio of band 3 to total protein concentration was determined in separate samples by covalently reacting band 3 with an EPR spin label, SL-H_2DADS-maleimide (Scothorn et al., 1996). This spin-

labeled stilbenedisulfonate derivative is specific for band 3, and its concentration was determined by comparing the doubly integrated linear EPR spectra of labeled band 3 and a spin-labeled standard (Scothorn et al., 1996). By this method, band 3 was determined to comprise ~36% of the BCA-detected protein in 5P7.4 ghosts obtained from the normal volunteer for these studies. EMA concentration was calculated from the absorbance at 532 nm, using an extinction coefficient of 104,000 M^{-1} cm^{-1} (Tsuji et al., 1988). Combining these two measurements gave the EMA:band 3 labeling stoichiometry. Although relative amounts of labeling can be accurately compared, systematic error could be introduced into the absolute labeling stoichiometry by any of the multiple measurements required. Considering the accuracy of the spin quantitation and assumed extinction coefficient for EMA, the overall determination should not be considered more accurate than ~10%.

Chromatographic procedures

Ion-exchange chromatography was performed with Fractogel TSK DEAE-650M support preequilibrated in DEAE running buffer (36 mM sodium phosphate, 0.1% $C_{12}E_8$, pH 7.4). Membrane samples were solubilized in 5 volumes of DEAE running buffer + 10% $C_{12}E_8$ and centrifuged as above. The supernatant was loaded onto DEAE and washed with >5 column volumes of running buffer, and then eluted stepwise by additions of buffer containing 100 mM NaCl (which eluted a minimal amount of EMA-labeled material) and 500 mM NaCl. The concentrated band of unstripped EMA-labeled band 3 was essentially completely eluted by this procedure, and was usually diluted fivefold in 5P7.4 + 0.1% $C_{12}E_8$ before HPLC size-exclusion chromatography. Some EDTA-stripped band 3 was retained on the column, and the EMA-labeled material was eluted in a larger volume, requiring that these samples be applied to the HPLC undiluted in 500 mM NaCl. Because the goal of this study is simply to measure the anisotropy of purified oligomeric species, quantitation of sample recovery was not pursued further.

Size-exclusion HPLC was performed by a modification of published procedures (Casey and Reithmeier, 1991). Samples were either DEAE-purified band 3, or membranes (stripped and unstripped) solubilized in HPLC solubilization buffer (5 mM sodium phosphate, 100 mM NaCl, 1% $C_{12}E_8$, pH 7.0), and centrifuged as above. Samples (100–500 μl at 0.5–2 mg/ml total protein concentration) were applied with a 500-μl loop to a 7.5 × 600 mm TSK-4000-SW size-exclusion column preequilibrated in HPLC running buffer (5 mM sodium phosphate, 100 mM NaCl, 0.2% $C_{12}E_8$, pH 7.0), at a 0.5 ml/min flow rate on a Waters HPLC system (Millford, MA). The eluate was monitored by EMA absorption at 532 nm. The void volume and included volume of the column were determined using blue dextran and β-mercaptoethanol standards (Sigma) in 5P7.0 + 100 mM NaCl. Some purified band 3 samples were dialyzed (24 h at 4°C, 50,000 MW cutoff) into 5P7.4 buffer containing 0.2% $C_{12}E_8$ before fluorescence measurements. All other samples were kept on ice until fluorescence spectroscopic experiments were performed, within 2 h of HPLC fractionation. The spectral centers of excitation measured in all $C_{12}E_8$-solubilized species were identical to within 1 nm, consistent with the EMA local environment not being significantly altered by trypsin treatment, EDTA stripping, or HPLC purification. The protein composition of HPLC fractions was determined by SDS-PAGE.

Optical spectroscopy

Steady-state fluorescence and anisotropy spectra were obtained on a SPEX 1681 Fluorolog (Edison, NJ) spectrofluorometer, using a 450-W xenon arc lamp for excitation. All spectra were corrected with a quantum counter reference. Unless otherwise noted, membrane samples were diluted to an optical density of less than 0.02 at 600 nm (~200-fold dilution from packed ghost pellets) to minimize the contribution of sample turbidity to fluorescence anisotropy. Sample turbidity caused by ghost membranes was found to decrease the anisotropy linearly by ~0.04 per OD unit at 600 nm (data not shown). The very dilute samples (EMA peak absorption of ~0.0005) also eliminate any inner filter effect (Lakowicz, 1983). Detergent-solubilized samples had essentially zero absorption at 600 nm. Background spectra were obtained immediately afterward from unlabeled samples of the same turbidity, or from HPLC running buffer (for HPLC-purified band 3). The background intensity was ~1–3% of the peak fluorescence intensity in most membrane samples, with a greater contribution in less intense regions of the spectrum and in substoichiometrically labeled samples. Single anisotropy values (e.g., Table 1) were obtained over collection times of 30–60 s for each polarizer orientation. The total intensity (S) and anisotropy (r) were calculated according to the standard equations,

$$S = I_{vv} + 2gI_{vh} \quad (1)$$

$$r = (I_{vv} - gI_{vh})/S \quad (2)$$

where I_{xy} represents the measured intensity (signal/reference − background/reference) with the excitation polarizer in orientation x and the emission polarizer in orientation y. The emission polarization bias (g-factor) was obtained using horizontally polarized excitation (I_{hv}/I_{hh}). Background subtraction accuracy was confirmed in excitation scans by observing that the g-factor was independent of excitation wavelength. Fluorescence quantum yield measurements were performed by comparing the total emitted photons of EMA with that of a fluorescein standard (in 0.1 M NaOH), and relative quantum yields were determined by comparing the absorption and fluorescence emission. For measurements at 37°C, the temperature was maintained by running water from a refrigerating/heating water bath through the water jacket of the cuvette holder, and the sample temperature was allowed to equilibrate 15 min before measurements. Absorption measurements were made on a Hewlett-Packard 8453 diode-array spectrophotometer.

Frequency-domain fluorescence lifetime and anisotropy measurements were made at the Laboratory for Fluorescence Dynamics (Urbana, IL), using a Spectra-Physics argon-ion laser for 514-nm excitation, and a Nd:YAG-pumped cavity dumped Coherent model 700 rhodamine dye laser for 570-nm excitation. Lifetime data were obtained with the emission polarizer rotated 54.7° (magic angle) from the vertical excitation, and were analyzed using a global nonlinear least-squares analysis package (Globals Unlimited, Urbana, IL). The g-factor was determined using horizontal excitation. Lifetime data were fit to a biexponential model in which one decay constant was fixed at 1 ps with a small (~0.5%) negative amplitude to account for a known instrumental artifact (T. H. Hazlett and E. Gratton, personal communication). Differential phase and modulation data were fit to a restricted-amplitude exponential decay model with a single correlation time and a nonzero residual anisotropy. Confidence intervals were generated by fixing a given parameter and allowing minimization to proceed over the remaining parameters (Beechem et al., 1991). Phosphorescence anisotropy data were obtained and analyzed as previously described (Blackman et al., 1996).

Contribution of concentration depolarization to homotransfer

At the high fluorophore concentrations encountered for EMA-labeled band 3 in the ghost membrane, nonspecific energy transfer can occur between nearby but unassociated band 3 oligomers (known as concentration depolarization). Numerous analytical models exist for calculating the magnitude of concentration depolarization (see Kawski, 1983; Bojarski and Sienicki, 1990; and Van der Meer et al., 1994, for reviews), which are limited in this case because of simplifying assumptions or the specific fluorophore configuration modeled. Some models could be adapted to modeling most aspects of the homotransfer in this particular situation (e.g., Wolber and Hudson, 1979), but to retain maximum flexibility, a Monte Carlo numerical approach was adopted. In each iteration, a random distribution of proteins was generated using known physical parameters for band 3, and the anisotropy decay due to homotransfer in the resulting distribution of fluorophores was calculated.

The calculation of homotransfer between two interacting fluorophores is given by (Tanaka and Mataga, 1979)

$$r(t) = \frac{1}{20}(6\cos^2\theta_{ae} + 3\cos^2\theta_{12} + 3\cos^2\theta_{21} - 4) + \frac{3}{20}(2\cos^2\theta_{ae} - \cos^2\theta_{12} - \cos^2\theta_{21})e^{-2k_T t} \quad (3)$$

where θ_{ae} is the angle between each fluorophore's absorption and emission dipole moments, and θ_{ij} is the angle between the ith fluorophore's absorption dipole and the jth fluorophore's emission dipole. The parameter k_T is the homotransfer rate, which depends on the intermolecular distance (R), the donor fluorescence lifetime (τ_D), and the characteristic distance (R_0):

$$k_T = \frac{1}{\tau_D}\left(\frac{R_0}{R}\right)^6 \quad (4)$$

R_0 is a function of the spectral properties of the chromophore as given by (Van der Meer et al., 1994)

$$R_0^6 = \frac{9000\ (\ln 10)\ \kappa^2 Q_D J}{128\ \pi^5 n^4 N_{AV}} \quad (5)$$

where κ^2 is the orientation factor, Q_D is the donor quantum yield, J is the overlap integral, n is the refractive index, and N_{AV} is Avogadro's number. The overlap integral J is calculated from the donor fluorescence (f_D) and acceptor absorption (ϵ_A) spectra:

$$J = \int_0^\infty f_D(\lambda)\epsilon_A(\lambda)\lambda^4 d\lambda \quad (6)$$

Of course, for homotransfer, "donor" and "acceptor" refer to the same species. The usual vector expression for κ^2 (e.g., equation 4.4 of Van der Meer et al., 1994) is parameterized as shown in Fig. 1, *A* and *B*. The orientations of each fluorophore's absorption and emission dipoles are defined by θ_a, θ_e, and ψ (Fig. 1 *A*), and geometry of the interacting pair is defined additionally by the intermolecular distance, R, and two azimuthal angles ω_1 and ω_2. Thereby the expression

$$\kappa_{12}^2 = \left\{\cos\theta_a\cos\theta_e - \frac{1}{2}\sin\theta_a\sin\theta_e[\cos(\omega_1 - \omega_2 + \psi) + 3\cos(\omega_1 + \omega_2 + \psi)]\right\}^2 \quad (7)$$

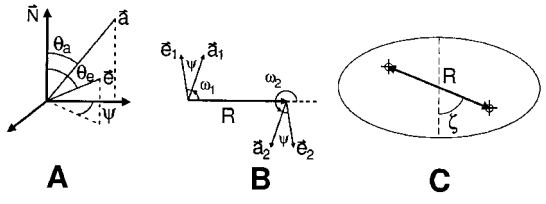

FIGURE 1 Definition of the angles used in modeling concentration depolarization. (*A*) A single fluorophore-labeled membrane protein is represented by the coordinate axis. The angles θ_a and θ_e are between the absorption and emission dipole vectors (**a** and **e**) and the membrane normal axis (N), and ψ is their azimuthal angle. (*B*) A pair of fluorophores as projected into the plane of the membrane. The angle ω_i is the azimuthal angle between the ith absorption dipole and the interfluorophore vector (**R**). In a C_2-symmetrical system as pictured, the difference ($\omega_2 - \omega_1$) is always equal to 180°. (*C*) The intermolecular distance **R** and the angle ζ define the positions of both fluorophores within the band 3 dimer (represented by the ellipse).

is obtained for forward transfer, with a similar expression with indices 1 and 2 switched for back transfer. It is readily calculated that κ^2 values for forward and back transfer are identical for a C_2-symmetrical fluorophore pair (in which $\omega_2 - \omega_1 = \pi$). The extension of Eq. 3 to multiple interacting fluorophores was derived as outlined by Tanaka and Mataga (1979).

Band 3 dimers in the simulation were represented as nonoverlapping ellipses with axis lengths of 110 Å and 55 Å. The dimensions of the ellipse were chosen to approximate the more irregular structure reported by electron microscopy (110 × 60 Å; Wang et al., 1994). This approximation overestimates the excluded volume of band 3, as indicated by the area being greater than the ~3000 Å^2 per dimer previously reported (Wang et al., 1994). Therefore, these calculations may underestimate the amount of concentration depolarization for band 3 in ghost membranes. To validate the randomness of the distribution, distribution functions were calculated from similar fields of circles, which agreed with published results (Zimet et al., 1995). Two fluorophores per dimer were located at arbitrary positions within the ellipse, subject to the following constraints: 1) C_2 symmetry of the dimer is maintained, 2) the probe orientation with respect to the membrane normal axis is fixed as previously determined (Blackman et al., 1996), and 3) the resulting intradimer homotransfer calculated according to Eq. 3, above, is consistent with the time-resolved anisotropy decay of dimeric band 3 (see Fig. 7). These constraints do not uniquely specify the position and orientation of the EMA fluorophores within the band 3 dimer. Two free parameters remain (Fig. 1, *B* and *C*): the angle ω (equal to $\omega_1 + \omega_2$), which is sufficient to fix κ^2 and thus R, and a second angle, ζ, which orients the interfluorophore vector within the elliptical band 3 dimer. The amount of concentration depolarization was at maximum for values of ω and ζ that positioned the fluorophores nearest to the ellipse border (ω such that R = 52 Å and ζ = 60°) and was at minimum when the fluorophores were deep within the ellipse (ω such that $R \approx 20$ Å and $\zeta = 0$).

RESULTS

Eosin homotransfer in band 3

The initial observation of EMA resonance energy homotransfer was made by noting the wavelength dependence of the fluorescence anisotropy. In the presence of homotransfer, excitation of a chromophore at the long-wavelength (red) edge of its excitation band results in a characteristic increase in the anisotropy, because homotransfer undergoes partial failure under low-energy excitation (Weber, 1960; reviewed in Demchenko, 1986). As shown in Fig. 2, band 3 stoichiometrically labeled with EMA exhibits a steady-state anisotropy of 0.28 (Fig. 2 *B*, *lower data set*) over much of the excitation spectrum (Fig. 2 *A*). However, approaching the red edge of the excitation band, the anisotropy increases to 0.33 at 575 nm as homotransfer progressively fails. To obtain good quality anisotropy data using red edge excitation, it was necessary to use a relatively high concentration of membranes (OD_{600} of ~0.5), which decreased the anisotropy by ~0.02 from its value in dilute ghosts (see Table 1). At the same concentration, ghost membranes solubilized in $C_{12}E_8$, which preserves band 3 dimeric structure as discussed below, are not turbid, but still exhibit a significant red edge effect, as shown in the middle data set. The upper data set in Fig. 2 *B* demonstrates that the red edge effect is greatly reduced when homotransfer is attenuated by substoichiometric (~12%) EMA labeling.

In a further investigation of EMA labeling stoichiometry, and of the structural requirements for homotransfer, the anisotropy was determined with 514-nm excitation, which

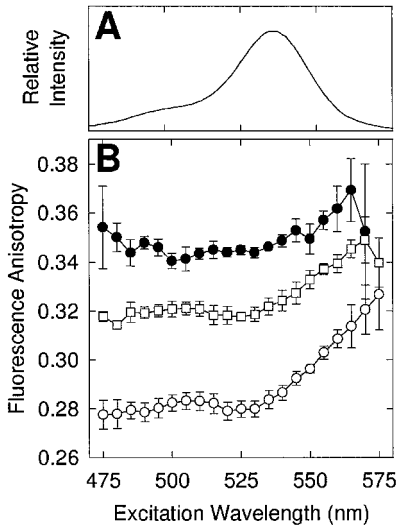

FIGURE 2 Failure of homotransfer under long-wavelength (red edge) excitation. (*A*) Excitation spectrum of EMA-labeled ghost membranes, which determines signal intensity. (*B*) Wavelength dependence of the membranes' steady-state fluorescence anisotropy. Displayed are data obtained from ghost membranes in 5P7.4 labeled at ~100% EMA:band 3 stoichiometry (○), from the supernatant after solubilization in $C_{12}E_8$ (□), and from membranes labeled at ~12% stoichiometry (●). All three data sets were obtained at room temperature at ~10-fold dilution from the concentration of packed membranes. Assuming that EMA labeling of dimers is a simple two-step, noncooperative, irreversible reaction, the fraction of EMA signal from doubly labeled band 3 is predicted to be ~12% in the substoichiometrically labeled sample.

is near the center of the excitation polarization spectrum and far from the red edge. The anisotropy of EMA-labeled ghost membranes decreases dramatically with increasing labeling stoichiometry (Fig. 3, *circles*) as a result of homotransfer. Under conditions of minimal labeling, which essentially eliminates homotransfer, the high anisotropy of 0.38 (close to the theoretical maximum of 0.4) indicates that there is no significant probe motion on the fluorescence (i.e., ns) time scale. Therefore, the prompt fluorescence anisotropy decay previously reported at a 1:1 labeling stoichiometry (Blackman et al., 1996) arises not from probe motion relative to the band 3 binding site, but from homotransfer. The approximate linearity of the data suggests that EMA binding/reaction is not strongly cooperative (see also Liu and Knauf, 1993); modeling the EMA reaction with dimeric band 3 as a two-step, irreversible reaction (not shown) predicts that significant positive or negative cooperativity would have been observed as an upward or downward concavity. EMA is well characterized and is used extensively as an affinity label for Lys^{430} of band 3 (Cobb and Beth, 1990); nevertheless, maximum labeling stoichiometry is reported as greater than 1:1. Although there is a small amount of nonspecific EMA labeling as indicated by SDS gel electrophoresis (see Discussion), the slight discrepancy likely arises from systematic errors in the stoichiometry determination.

Other data in Fig. 3 indicate that homotransfer is dependent on an intact protein structure, because the stoichiometry dependence is eliminated when band 3 is denatured and dimers are disrupted by boiling in 1% SDS + 5 mM dithiothreitol (Fig. 3, *triangles*). The decreased (but stoichiometry-independent) anisotropy in SDS most likely reflects increased probe motion resulting from band 3 denaturation. Finally, measurements were performed on unstripped ghosts solubilized in 1% $C_{12}E_8$ (Fig. 3, *squares*), a nonionic detergent that preserves important features of band 3 structure, including its dimeric structure (Casey and Reithmeier, 1991). As expected, the limiting anisotropy at low stoichiometry (0.38) and the excitation spectral center were essentially unchanged by solubilization, consistent with the local environment of EMA not being significantly perturbed. Interestingly, however, the stoichiometry dependence of the anisotropy was attenuated after solubilization, indicating an overall decrease in homotransfer. The important differences between the samples lie in the different classes of homotransfer. The $C_{12}E_8$-solubilized band 3 is entirely dimeric according to size-exclusion HPLC (see Fig. 5 *C*), so homotransfer can occur only within dimers at the submicromolar band 3 concentration used in this experiment. Two additional contributions to homotransfer may be present in ghost membranes. First, band 3 in the ghost membranes may be more highly oligomerized, with additional intramultimer homotransfer occurring. Second, band 3 is more locally concentrated (~3 mM in the membrane), indicating that nonspecific homotransfer between nearby but unassociated oligomers (concentration depolarization) may also be occurring. This initial finding prompted a more detailed investigation relating the level of homotransfer and band 3 self-association, which is described below.

It is important to consider other phenomena that might affect the steady-state anisotropy. For instance, changes in the fluorescence lifetime could have a significant effect on the anisotropy. Because homotransfer per se does not affect the lifetime or quantum yield, such changes would be indicative of another process, such as quenching. The lifetime of EMA-labeled band 3 was measured in intact ghosts and in $C_{12}E_8$ solution and is shown in Fig. 4. Multiple data sets obtained over a 100-fold range in labeling stoichiometry overlaid almost perfectly (Fig. 4 *A*). The best-fit lifetimes were single exponential decays, independent of labeling stoichiometry, and similar between solubilized and unsolubilized samples (Fig. 4 *B*). The lifetimes were also stoichiometry-independent by red edge excitation at 570 nm (average values 2.90 ns for ghosts, 3.16 ns in $C_{12}E_8$; data not shown). The eosin lifetime in fully labeled erythrocyte ghosts (2.98 ns) was similar to previously reported results of 2.99 ns (Macara et al., 1983) and 3.2 ns (Bicknese et al., 1995). The slight lifetime change upon $C_{12}E_8$ solubilization is too small and, moreover, is in the wrong direction to explain the significant anisotropy differences between the solubilized and unsolubilized samples. The fluorescence quantum yield was also independent of labeling stoichiometry (not shown), indicating that self-quenching is not a significant concern in this system. In intact ghosts, the centers of the excitation and emission spectra are also

TABLE 1 Anisotropy values obtained using 488-nm excitation for various preparations of EMA-labeled band 3

Sample	Buffer	Temperature	Anisotropy (mean ± SD)
Ghost membranes	5P7.4	37°C	0.302 ± 0.003
Ghost membranes + 5.3 μM melittin	5P7.4	37°C	0.252 ± 0.005
Ghost membranes	10 mM HEPES pH 7.4	37°C	0.291 ± 0.006
Ghost membranes + 0.5 mM $ZnCl_2$	10 mM HEPES pH 7.4	37°C	0.212 ± 0.009
Trypsin-treated ghost membranes	5P7.4	37°C	0.300 ± 0.002
$C_{12}E_8$-solubilized ghosts	5P7.4 + 0.2% $C_{12}E_8$	RT*	0.319 ± 0.003
$C_{12}E_8$-solubilized trypsin-treated ghosts	5P7.4 + 0.2% $C_{12}E_8$	RT	0.322 ± 0.004
HPLC-purified dimeric band 3 (unstripped)	5P7.4 + 0.2% $C_{12}E_8$	RT	0.317 ± 0.003
HPLC-purified dimeric band 3 (EDTA-stripped)	5P7.4 + 0.2% $C_{12}E_8$	RT	0.322 ± 0.002
HPLC-purified tetrameric band 3	5P7.4 + 0.2% $C_{12}E_8$	RT	0.295 ± 0.007
HPLC-purified aggregated band 3	5P7.4 + 0.2% $C_{12}E_8$	RT	0.294 ± 0.016
$C_{12}E_8$-solubilized ghosts	5P7.0 + 100 mM NaCl + 0.2% $C_{12}E_8$	RT	0.288 ± 0.004
HPLC-purified dimeric band 3 (unstripped)	5P7.0 + 100 mM NaCl + 0.2% $C_{12}E_8$	RT	0.284 ± 0.004
HPLC-purified dimeric band 3 (EDTA-stripped)	5P7.0 + 100 mM NaCl + 0.2% $C_{12}E_8$	RT	0.279 ± 0.004
HPLC-purified tetrameric band 3	5P7.0 + 100 mM NaCl + 0.2% $C_{12}E_8$	RT	0.266 ± 0.013
HPLC-purified aggregated band 3	5P7.0 + 100 mM NaCl + 0.2% $C_{12}E_8$	RT	0.258 ± 0.009
HPLC-purified dimeric trypsin-treated band 3 (unstripped)	5P7.0 + 100 mM NaCl + 0.2% $C_{12}E_8$	RT	0.288 ± 0.001

*RT indicates room temperature, which was usually 24°C, but varied from ~23°C to 27°C.

stoichiometry-independent, the latter ruling out a significant reabsorption-mediated transfer. The EMA labeling specificity, as measured by SDS-PAGE, was independent of labeling stoichiometry (not shown), ruling out potential alternative explanations such as the differential labeling of nonspecific, high-mobility sites.

After demonstrating the existence of resonance energy homotransfer in band 3, the effective distance range was estimated. The distance at which homotransfer is at half-maximum, given by the R_0 parameter (Eq. 5), was calculated from EMA spectral properties such as the extinction coefficient (104,000 M^{-1} cm^{-1}; Tsuji et al., 1988), quantum yield (0.15; data not shown), and overlap integral (2.50×10^{-13} M^{-1} cm^3; data not shown). EMA-band 3 has a small Stokes shift (excitation peak 530 nm, emission peak 550 nm) contributing to its relatively large R_0 value of 42 Å, even assuming a suboptimal case of chromophore geometry ($\kappa^2 = 2/3$). The R_0 could be as large as 57 Å at the optimal geometry ($\kappa^2 = 4$), giving significant homotransfer (20% efficiency) as far as 72 Å. These distances are comparable to the dimensions of the band 3 dimer (Wang et al., 1993), suggesting that homotransfer could occur between subunits in a multimer, as well as between monomers in a dimer. Thus association of band 3 dimers into larger oligomers would be expected to increase EMA homotransfer.

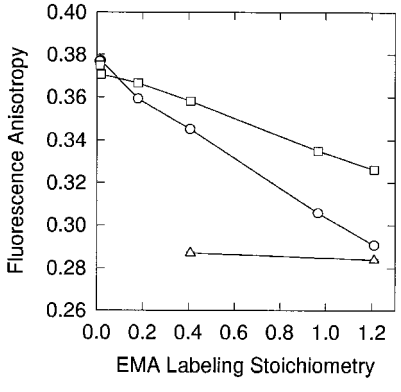

FIGURE 3 Effect of labeling stoichiometry on the EMA fluorescence anisotropy. Data were obtained using 514-nm excitation on suspensions of erythrocyte ghost membranes diluted 50-fold in 5P7.4 (○), the supernatant from $C_{12}E_8$-solubilized membranes (□), and membranes boiled in 5P7.4 + 1% SDS + 5 mM dithiothreitol (△). Labeling stoichiometry was determined from EMA absorbance and the total protein concentration as outlined in Materials and Methods.

Homotransfer reports on band 3 oligomeric state

To conclusively show that homotransfer is sensitive to band 3 oligomerization, anisotropy measurements were performed in samples that exhibit only intradimer and intramultimer homotransfer, and do not exhibit concentration depolarization. This requirement is met by purified stable oligomers of $C_{12}E_8$-solubilized band 3, which were isolated by published procedures (Casey and Reithmeier, 1991). EMA-labeled, EDTA-stripped ghost membranes were solubilized in $C_{12}E_8$ and purified by DEAE chromatography and size-exclusion HPLC. As shown in Fig. 5, elution profiles of EMA-labeled material (detected at 532 nm) were very similar to those reported previously for unlabeled band 3 at 215 and 280 nm detection (Casey and Reithmeier, 1991). Three species of increasing Stokes radius were isolated by solubilizing ghost membranes stripped of their cytoskeletal proteins (Fig. 5, *curve a*). By comparing retention times with the single symmetrical peak eluted from solubilized unstripped ghosts (*curve c*), the last EMA-labeled species to elute from the column was identified as dimeric band 3. The two larger species are attributed, as in the earlier work, to band 3 tetramers and aggregates (see Casey and Reithmeier, 1991, for further discussion). Most

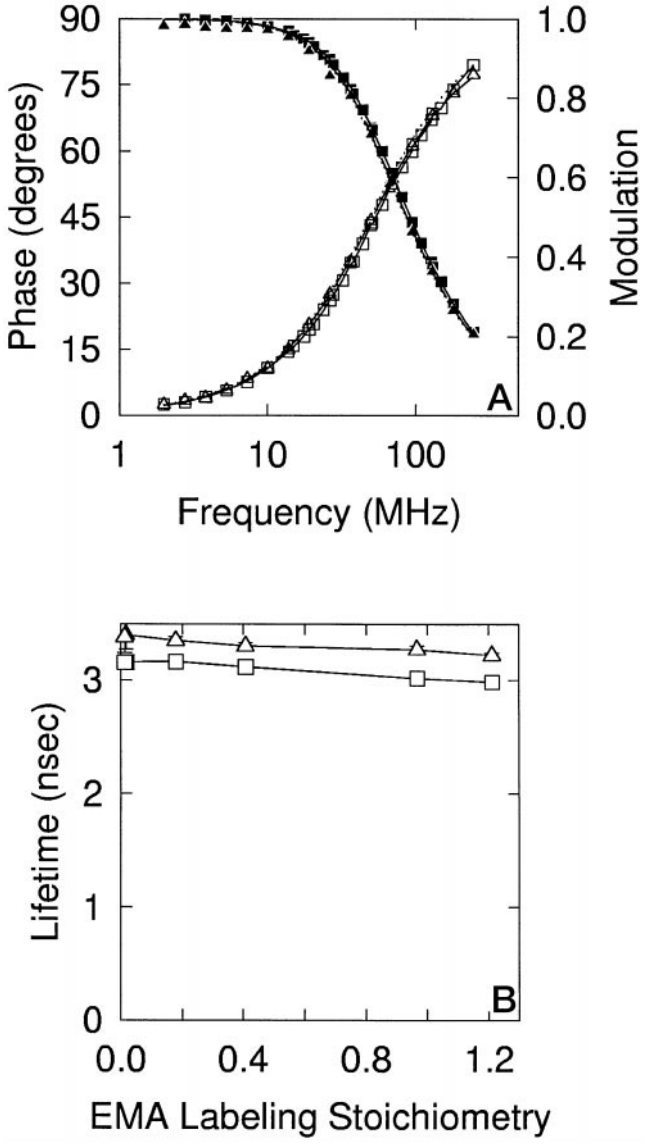

FIGURE 4 Measurement of the fluorescence lifetime of EMA-band 3 versus labeling stoichiometry. (*A*) Phase (*empty symbols*) and modulation (*filled symbols*) data sets were obtained using 514-nm excitation on 50-fold diluted ghost membranes that had been labeled with EMA at six different stoichiometries. For clarity, data and fits are shown only for the highest (~100% labeling; *squares* and *solid line*) and lowest (~1% labeling; *triangles* and *dashed line*) stoichiometries; the intermediate samples are essentially identical. The same experiment was performed on the supernatants of $C_{12}E_8$-solubilized ghost membranes, and the fits for the highest stoichiometry are shown (*dotted line*), with the data points omitted. (*B*) Fit parameters for EMA-labeled intact ghosts (□) and $C_{12}E_8$-solubilized ghosts (△) plotted versus labeling stoichiometry. Error bars (hidden by the symbols for all except the lowest stoichiometries) represent 68% confidence intervals. Fit parameters are as follows: for stoichiometries of 1.21, 0.97, 0.41, 0.18, 0.02, 0.01, intact membrane lifetimes are 2.98, 3.04, 3.11, 3.17, 3.16, and 3.16 ns; $C_{12}E_8$-solubilized membranes lifetimes are 3.22, 3.27, 3.30, 3.35, 3.40, and 3.38 ns.

samples were rechromatographed after fluorescence measurements to verify their purity and stability (e.g., *curve b*), and separate HPLC experiments indicated that the purified oligomers were stable at least 1 day after purification. The

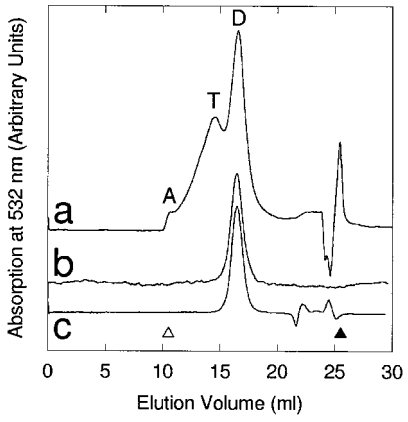

FIGURE 5 HPLC elution profiles from a 7.5 × 600 mm TSK-4000-SW size exclusion column, detected by EMA absorbance at 532 nm. (*a*) $C_{12}E_8$-solubilized, EDTA-stripped ghost membranes purified by DEAE chromatography. (*b*) Rechromatography of HPLC-purified dimeric band 3, which was DEAE-purified from stripped ghost membranes. (*c*) Unstripped ghost membranes applied directly to the HPLC column after $C_{12}E_8$ solubilization. In curve a, the major species are labeled as follows: D, band 3 dimers; T, putative tetramers; A, putative aggregates. Arrowheads mark the elution positions of blue dextran (△; void volume) and β-mercaptoethanol (▲; included volume). The feature occurring at ~25 ml in curve a is due to the 500 mM NaCl in which this sample was injected, and contained neither Coomassie-stainable protein nor EMA fluorescence. In curve c, the features at ~22 ml and 25 ml occurred in samples that were not DEAE-purified, did not contain detectable protein or EMA fluorescence, and are believed to represent detergent micelles and/or lipid-containing micelles.

anisotropy of the purified oligomers (488-nm excitation; Table 1) show that larger oligomers have a progressively lower anisotropy as the species size increases. The absolute values of the anisotropy varied in some preparations by as much as 0.03, but within each preparation, the dependence of anisotropy on Stokes radius was always observed. Anisotropy measurements of the samples dialyzed back into NaCl-free buffer (5P7.4 + 0.2% $C_{12}E_8$) also indicated that tetrameric and aggregated band 3 had a lower anisotropy than dimeric band 3. It was noted in these studies that 100 mM NaCl (required for HPLC purification) decreased the anisotropy of all EMA-labeled band 3 species, including ghost membranes, $C_{12}E_8$-solubilized membranes, and HPLC-purified oligomers. The dose-response curve for NaCl was hyperbolic, with an apparent K_D of ~60 mM, in substoichiometrically labeled samples as well as fully labeled samples (not shown). This indicates that the anisotropy decrease is not due to homotransfer, but could represent nanosecond time scale segmental protein motions (see Bicknese et al., 1995, for further discussion). Collectively, these data show that EMA homotransfer is sensitive to the band 3 oligomeric state.

Detection of band 3 oligomeric state in the intact membrane

Homotransfer was found to be sensitive to the band 3 oligomeric state in the intact erythrocyte ghost membrane.

Two agents known to induce clustering of band 3 in membranes are zinc ions (e.g., Clague and Cherry, 1989; Turrini et al., 1991) and melittin (e.g., Clague and Cherry, 1989; Hui et al., 1990). To test whether EMA homotransfer is altered by this clustering, intact erythrocyte ghost membranes were incubated with varying concentrations of each of these agents, and the fluorescence anisotropy was measured. For $ZnCl_2$, the anisotropy decreased dramatically with increasing Zn^{2+} concentration, following a hyperbolic curve with an effective K_D of 54 μM. Therefore, Zn^{2+} has roughly the same potency for altering homotransfer as in previous studies of rotational mobility (Clague and Cherry, 1989). The anisotropy decrease was at maximum at ~0.5 mM $ZnCl_2$ (Fig. 6 *B* and Table 1), where phosphorescence anisotropy data (Fig. 6 *A*) indicated complete immobilization of band 3. The addition of 1 mM NaCl instead of $ZnCl_2$ had no effect on the anisotropy (not shown), ruling out potential effects of chloride anions. Both the phosphorescence and fluorescence anisotropies were similar to pretreatment values when the zinc was chelated by adding 113cit7.4, and the samples were washed back into zinc-free HEPES buffer, indicating that zinc-induced association is reversible. This is critical for making comparisons with any clusters in the native membrane, because only a small amount of stable aggregate is reported by size-exclusion HPLC (Casey and Reithmeier, 1991, and Fig. 5). The anisotropy exhibited a time-dependent decrease over several hours, from 0.234 (immediately after $ZnCl_2$ addition) to a plateau value of 0.212; sample turbidity increased insignificantly over this time, and reversibility was complete even after this extended treatment with zinc. The total intensity of zinc-treated samples was decreased by ~10%, suggesting that a quenching process might be contributing. However, a dynamic quench would increase the anisotropy, the opposite of what is observed. The center of the excitation spectrum was red-shifted only by 0.5 nm, suggesting no significant changes in the chromophore environment. The same experiment, when repeated on ghosts labeled at ~30% EMA: band 3 stoichiometry, showed a greatly attenuated anisotropy change (~0.03), consistent with homotransfer being the source of the fluorescence anisotropy changes. The anisotropy of zinc-treated samples was independent of a twofold variation in membrane concentration, indicating that a small increase in turbidity of zinc-treated membranes (OD change at 600 nm < 0.02) does not significantly affect the anisotropy.

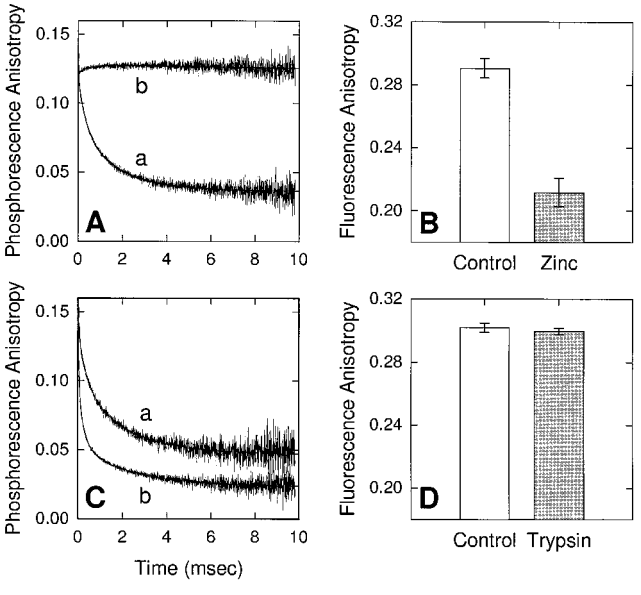

FIGURE 6 Comparison of rotational diffusion and homotransfer measurements. (*A*) Time-resolved phosphorescence anisotropy data obtained from stoichiometrically EMA-labeled ghosts at 37°C, deoxygenated in 10 mM HEPES buffer, pH 7.4. The lower decay (*a*) is from ghost membranes diluted in buffer alone, and the upper decay (*b*) is from ghosts diluted in buffer + 0.5 mM $ZnCl_2$. (*B*) Steady-state fluorescence anisotropy obtained for samples treated as in *A*, except that they were not deoxygenated. (*C*) Time-resolved phosphorescence anisotropy data obtained from stoichiometrically EMA-labeled ghosts at 37°C, deoxygenated in 5P7.4 buffer. The upper decay (*a*) is from unproteolyzed ghost membranes, and the lower decay (*b*) is from trypsin-treated ghosts. (*D*) Steady-state fluorescence anisotropy obtained for samples treated as in *C*, except that they were not deoxygenated.

The same results were obtained in separate experiments, using melittin as the clustering agent. The dose-response data for the fluorescence anisotropy were sigmoidal, with a half-maximum effect at ~1.4 μM melittin and a maximum effect by 5.3 μM (Table 1). Phosphorescence data obtained using 0.17 μM and 5.3 μM melittin (not shown) showed ~5% (judged by the increase in r_∞) and 100% immobilization over 10 ms, in agreement with the homotransfer dose-response data. Substoichiometrically labeled samples treated with melittin showed a greatly attenuated anisotropy change (~0.01), consistent with homotransfer being the source of the fluorescence anisotropy changes. Interestingly, higher concentrations of melittin resulted in a smaller, progressive rise in the plateau anisotropy value ($r = 0.268$ at 55 μM), suggesting that the excess melittin molecules may intercalate into the band 3 clusters, reducing the amount of homotransfer (see the model discussed in Clague and Cherry, 1989).

Effect of mild trypsin treatment on band 3 self-association

The above data clearly show that because of homotransfer, the fluorescence anisotropy of EMA-labeled band 3 is sensitive to changes in its oligomeric state, both in detergent solution and in the intact membrane. This immediately invites the comparison with rotational diffusion studies of EMA-labeled band 3 performed under similar conditions. For instance, the apparent rotational mobility of a slowly rotating population of band 3 is significantly increased after proteolytic removal of its cytoplasmic domain (Nigg and Cherry, 1980). This finding has been repeated in many laboratories, including our own (Fig. 6 *C*). To determine whether this change in rotational mobility corresponds to a change in the in situ oligomeric state of band 3 (as discussed

in Nigg and Cherry, 1980; Clague et al., 1989; Wyatt and Cherry, 1992), the anisotropies of trypsin-treated and untreated ghosts in 5P7.4 were compared (Table 1) and found to be identical. The anisotropy of 100% clustered band 3 (represented by zinc-treated ghosts) has already shown that a change in oligomerization, especially one of the magnitude inferred from optical rotational dynamics data, would be readily detectable if present. Subsequent SDS-PAGE analysis (not shown) ruled out the possibility of proteolysis during the ~30-min course of this experiment. This indicates that, in ghost membranes at 37°C, the self-association of band 3 is not altered by its prior cleavage from its cytoskeletal attachment.

Calculation of concentration depolarization

Before addressing the question of whether a significant fraction of band 3 is in clusters larger than tetramers in the intact membranes, the contribution of homotransfer between unassociated band 3 oligomers (concentration depolarization) must be calculated. Various analytical models examined (Wolber and Hudson, 1979; others reviewed by Kawski, 1983; Bojarski and Sienicki, 1990; Van der Meer et al., 1994) are in agreement that, at the high density of band 3 dimers in ghost membranes, concentration depolarization should contribute significantly to the fluorescence depolarization. Concentration depolarization depends on parameters (see Materials and Methods) that are known or may be estimated for band 3 in ghost membranes. Some parameter values come from the frequency-domain anisotropy measurements shown in Fig. 7 for $C_{12}E_8$-solubilized band 3, which is dimeric (Fig. 5 *C*) and is too dilute to exhibit concentration depolarization. The fit in Fig. 7 is to a single correlation time of restricted amplitude, which is expected for homotransfer in dilute fluorophore pairs (Eq. 3). The homotransfer rate, k_T, is calculated to be 0.5 ns^{-1}, which fixes the relationship between κ^2 and R (Eq. 4), because the donor lifetime, τ_D, and the characteristic distance, R_0, are known. The initial and final anisotropy values constrain the possible fluorophore orientations within the dimer (Eq. 3), and one of the symmetry-related possibilities is nearly identical to a previous independent measurement (Blackman et al., 1996): $\theta_a = 69°$, $\theta_e = 82°$, $\psi = 0°$. Finally, the number density of band 3 within the membrane (Fairbanks et al., 1971; discussed in Jennings, 1984) is 10^6 per erythrocyte, or ~7500 dimers/μm^2. Using the model outlined above, the contribution of concentration depolarization to the anisotropy of dimeric band 3 in ghost membranes occurring can be calculated for any given values of the two free parameters (ω and ζ). When the two parameters are allowed to vary over physically possible values, the amount of concentration depolarization ranges from ~0.005 to 0.016.

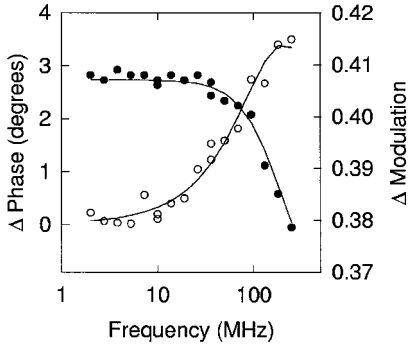

FIGURE 7 Frequency-domain anisotropy measurement of $C_{12}E_8$-solubilized membranes. Overlaid are the differential phase (○) and modulation (●) data sets obtained using 514 nm excitation on the supernatant of $C_{12}E_8$-solubilized membranes, diluted to an OD_{532} of ~0.002 in 0.1% $C_{12}E_8$. The lines illustrate a simultaneous fit to the equation $r(t) = (r_0 - r_\infty)\, e^{-t/\phi} + r_\infty$. Fit parameters are $r_0 = 0.37$ [0.365, 0.377]; $r_\infty = 0.31$ [0.309, 0.316]; $\phi = 1.0$ ns [0.8, 1.3]. Brackets denote 68% confidence intervals.

Determination of band 3 oligomeric state in situ

We can now use the steady-state anisotropy data in Table 1 to calculate the fraction of clustered band 3 in ghost membranes at 37°C. To accomplish this, a simplified model of band 3 self-association is used, in which it is assumed that band 3 consists of a linear combination of oligomers whose anisotropy values are known; in this situation, the observed anisotropy value for the mixture is the weighted average of the values determined for the components (Table 2). Based on reports in the literature documenting the existence of a tetrameric band 3 species (e.g., Casey and Reithmeier, 1991; Weinstein et al., 1980), the first two models contain dimeric, tetrameric, and highly clustered band 3. The weighted average was constrained by using a 70:30 ratio of dimers:tetramers (Casey and Reithmeier, 1991). Using the anisotropy value for tetramers purified and dialyzed into 5P7.4 (Tet_A), the fraction of clustered band 3 required to explain the residual amount of homotransfer is 9.9%, as shown. An alternative value for the anisotropy of tetramers (Tet_B) was calculated from HPLC-purified tetramers in 100 mM NaCl, after correcting for the effect of NaCl measured

TABLE 2 Calculation of the fraction of highly clustered band 3 from fluorescence anisotropy data

	Clustered fraction, using:		
Components	Conc. dep. = 0	Conc. dep. = 0.005	Conc. dep. = 0.016
Dim + Tet_A + Clust	9.9 ± 0.3%	5.2 ± 0.3%	0.0%
Dim + Tet_B + Clust	10.3 ± 0.8%	5.6 ± 0.8%	0.0%
Dim + Agg	15.9 ± 0.2%	11.8 ± 0.2%	1.2 ± 0.2%

The anisotropy value for dimers was taken from the supernatant of $C_{12}E_8$-solubilized ghosts (0.319), and the value for large clusters was taken from zinc-treated ghost membranes (0.212). The values for tetramers were taken from HPLC-purified, dialyzed tetramers (Tet_A; 0.295), and from the HPLC-purified tetramers in 100 mM NaCl, corrected by 0.031 for the effect of 100 mM NaCl on dimeric band 3 (Tet_B; 0.297). In the third column, both 0% fractions are obtained for all values greater than Conc. dep. = 0.010. Uncertainties in these values were obtained by propagating the errors in the anisotropy values through the calculation.

in dimeric band 3; the resulting clustered fraction is only slightly greater. Because band 3 "tetramers" in $C_{12}E_8$ have been much less well characterized than dimers, the anisotropy of the purified species may not accurately reflect that of tetramers in the membrane. Therefore, a third calculation is presented, postulating that band 3 in membranes is solely dimeric and highly clustered. This provides a rough upper limit of 15.9% on the fraction of clusters compatible with these homotransfer data. Although uncertainties for these values are reported in Table 2, it should be kept in mind that a larger potential source of error is the choice of basis set of anisotropy values. These calculations, which still ignore the effect of concentration depolarization, indicate a fraction of clustered band 3 that is clearly much lower than optical rotational diffusion data have suggested (e.g., Corbett and Golan, 1993).

When concentration depolarization is included, the amount of unattributed homotransfer that could arise from clustering is even less. The second and third columns of Table 2 show results for incorporating concentration depolarization as calculated by the Monte Carlo simulation described earlier, with the minimum and maximum values obtained by allowing the two free parameters (ω and ζ) to take all of their possible values. When the minimum amount of concentration depolarization is included, less than 5% highly clustered band 3 must be postulated to explain the residual amount of homotransfer. For about half of the possible values of concentration depolarization, the fraction of clustered band 3 needed to fit the observations is 0%. The main finding for all of the models presented is that homotransfer data in ghost membranes at 37°C can be explained by dimeric and tetrameric band 3 without including any substantial clustered fraction of band 3.

DISCUSSION

Band 3 oligomerization is thought to be an important determinant of erythrocyte membrane structure and function. Many techniques, including spectroscopic measurements of rotational diffusion (e.g., Matayoshi and Jovin, 1991; Hustedt and Beth, 1995), target size analysis (Cuppoletti et al., 1985), freeze-fracture electron microscopy (e.g., Weinstein et al., 1980), and chemical cross-linking (e.g., Steck, 1972; Staros and Kakkad, 1983), have yielded information on band 3 oligomerization in the intact erythrocyte ghost membrane. Although each technique has provided valuable data, significant apparent discrepancies have confused the general picture of band 3 oligomerization in situ (discussed in Jennings, 1984). In this work we report the existence of resonance energy homotransfer in band 3 labeled on the transmembrane domain with eosin-5-maleimide, and its application as a valuable tool for probing band 3 oligomeric state in the intact membrane. Homotransfer has already been shown to be useful for measuring protein structure (e.g., Bastiaens et al., 1992) and oligomerization (e.g., Runnels and Scarlata, 1995). In the latter work, a detailed theoretical and experimental study indicated that homotransfer is sensitive to oligomerization when the dimensions of the monomers are less than $\sim 2R_0$. Transition dipole orientations were not included in their theory, but a good agreement was found with the experimental data for that system. Just as for heterotransfer, it is possible for an unfavorable probe orientation to significantly reduce the efficiency of homotransfer. In band 3, the EMA molecules are immobilized, oriented, and isolated from each other (indicated in this work by the absence of any self-quenching). We have shown that these additional factors do not deter using homotransfer to measure oligomerization. A significant advantage of homotransfer over heterotransfer experiments is that, for complex systems such as band 3 in ghost membranes, obtaining a well-defined population of labeled proteins is generally made much simpler by employing one spectroscopic label rather than two (also discussed in Karolin et al., 1998). Another advantage of using energy transfer is that it senses the proximity only of labeled band 3 molecules, meaning that it is insensitive to interactions with unlabeled proteins such as ankyrin (Bennett and Stenbuck, 1979), glycophorin (Che and Cherry, 1995), or band 4.2 (Golan et al., 1996; Rybicki et al., 1996), unless those interactions change the relative disposition of two or more band 3 proteins. Therefore, as a new assay for the dimensions of band 3 oligomers, homotransfer provides information complementary to other techniques such as rotational dynamics measurements. Proteolytic cleavage of the membrane and cytoplasmic domains results in a large change in band 3 mobility, as reported by triplet-state optical spectroscopic techniques (Nigg and Cherry, 1980; Matayoshi and Jovin, 1991; Blackman et al., 1996), but it has remained unclear whether the change arises from the disruption of band 3 clusters, or from a release of band 3, which is directly restricted by its interaction with ankyrin and the cytoskeleton. In this report, homotransfer measurements clearly show that band 3 self-association at 37°C is not changed by prior trypsin proteolysis. Furthermore, in a comparison of data from ghost membranes with those from purified dimeric, tetrameric, and highly clustered band 3, a fraction of clustered band 3 is not required to interpret the data. This strongly suggests that interpretations of rotational diffusion in terms of a significant fraction of large clusters should be reevaluated in terms of alternative dynamic models. One feature that can now be examined in more detail is the tether between band 3 and the cytoskeleton, whose importance in determining the stability and flexibility of the erythrocyte membrane was cited in the Introduction. Because a significant fraction of clustered band 3 can be ruled out, certain features in the optical anisotropy decays—in particular, the amount of residual anisotropy after long times—can be interpreted in terms of the effect of a cytoskeletal tether.

Resonance energy homotransfer in EMA-labeled band 3

Resonance energy transfer between fluorescently labeled band 3 proteins in the erythrocyte membrane can be classi-

fied into three general categories. Intradimer transfer occurs within the symmetrical band 3 dimer; interdimer transfer can occur within higher-order oligomeric complexes (intramultimer); or it can arise because of the crowding of band 3 at high concentrations in the intact membrane (concentration depolarization). While quantitation of intramultimer transfer is required to draw conclusions about the association state of band 3 beyond dimeric complexes, the occurrence of at least intradimer homotransfer in EMA-labeled band 3 is reasonable, given the dimensions of the band 3 dimer (110 × 60 Å in cross section; Wang et al., 1994) and previous results demonstrating both resonance energy homotransfer and heterotransfer in fluorescently labeled band 3 (Dissing et al., 1979; Macara and Cantley, 1981). The former report of Dissing et al. used homotransfer between labeled cytoplasmic domains of band 3 to demonstrate its dimeric state in vesicles stripped of other membrane and cytoskeletal proteins, but did not delineate the possible sources of interdimer homotransfer. This work, in contrast, uses the interdimer component to measure the higher-order associations of band 3 dimers. The latter report of Macara and Cantley placed the distance between EMA and a stilbenedisulfonate anion exchange inhibitor at 29–52 Å, and noted that interdimer transfer might also be occurring. The partial overlap of EMA and stilbenedisulfonate binding sites (Cobb and Beth, 1990) suggests that the intradimer distance between EMA binding sites is similar. Given that the distance for half-maximum EMA homotransfer, R_0, is calculated to be as great as 57 Å (depending on the fluorophore geometry), the observation of homotransfer in EMA-band 3 is quite reasonable on theoretical grounds.

To use homotransfer to reach the goal of this work, the assessment of the oligomeric state of band 3 in situ, it is necessary to make sure the fluorescence anisotropy is reporting homotransfer and not other factors. Anisotropy is sensitive to many phenomena, including probe rotational motion, electronic properties of the chromophore (e.g., fluorescence decay time), and homotransfer. Fig. 3 rules out a significant contribution of rotational motion (which is independent of labeling stoichiometry). Although the theoretical possibility of a cooperative, stoichiometry-dependent probe motion cannot be directly ruled out in this work, such a change in probe orientation has been ruled out by confocal microscopy (Blackman et al., 1996; and Blackman, Piston, and Beth, unpublished), arguing strongly against a similar change in probe motion. Fig. 4 shows that anisotropy changes are independent of fluorescence decay time. Thus, all of the indications are that the stoichiometry-dependent anisotropy changes in EMA-labeled band 3 are due solely to homotransfer.

The maximum labeling stoichiometry in this study was 1.1–1.2 EMA per band 3 monomer (e.g., Fig. 3). This slight apparent excess of labeling may arise from systematic errors in the multistep stoichiometry determination. However, some nonspecific labeling may exist, even though EMA is extremely well characterized to be more than 90% specific for Lys-430 of band 3 (Nigg and Cherry, 1979b; Cobb and Beth, 1990). Examination of overexposed fluorescence images of SDS gels (not shown) shows two faint EMA-labeled bands, migrating at ~62 kDa and ~24 kDa, whose fluorescence in substoichiometrically labeled samples is reduced approximately proportionally to band 3. The larger MW band has a mobility similar to that of the 60-kDa chymotryptic fragment of band 3 (e.g., Jennings and Nicknish, 1985), indicating that perhaps only the smaller band represents a nonspecific labeling target. These observations do not affect results obtained in HPLC-purified band 3. However, in unpurified samples, it is important to consider whether features smaller than ~10% of the total fluorescence signal could arise from a nonspecific labeling component. In this work, most changes observed in unpurified band 3 surpass this threshold and are supported by similar results obtained in HPLC-purified band 3. At the opposite extreme, the lack of anisotropy change upon trypsin treatment (Fig. 6 *D*, Table 1) cannot reasonably be attributed to nonspecific labeling.

Homotransfer reports on band 3 self-association

In the presence of homotransfer, the fluorescence anisotropy is dependent on the distance and relative orientation of one probe with respect to its symmetry-related partner within the dimer, and on the number of available partners in other dimers. If the orientation and interprobe distance are unaltered, then an anisotropy change directly reflects a change in protein oligomerization. Previous work by Casey and Reithmeier (1991) showed that stable band 3 species, with physical properties consistent with dimers, tetramers, and aggregates of $C_{12}E_8$-solubilized band 3, could be isolated by size-exclusion HPLC. Fig. 5 shows that essentially the same EMA-labeled band 3 species can be isolated by the same procedures. The dependence of the anisotropy on the size of the oligomeric species (Fig. 6 *D*, Table 1) shows that homotransfer increases as band 3 dimers associate to form larger oligomers. This demonstrates the presence of intramultimer homotransfer.

Homotransfer measurements of oligomerization in situ

The studies in nondenaturing detergent demonstrate that homotransfer increases progressively for larger band 3 oligomers, and the results from zinc and melittin studies (Table 1) indicate that the same is true in the intact ghost membrane. The significant anisotropy changes upon clustering band 3 indicate that greater than 5–10% clustered fractions should be readily observable. The demonstration that EMA homotransfer at 37°C is unaffected by prior trypsin proteolysis (Table 1) clearly indicates that band 3 self-association is unchanged. This suggests that interaction with the cytoskeleton restricts the amplitude of band 3 rotational diffusion but does not change its self-association state. A model that also includes a flexible link between band 3 and

the cytoskeleton was discussed by Hustedt and Beth (1995), and is generally consistent with both optical and ST-EPR rotational diffusion data, as well as the data in Table 1. It is unclear at this point why trypsin-treated tetramers do not appear to be disrupted in the membrane, although hypothetically a weak association could remain that is disrupted by HPLC chromatography (Casey and Reithmeier, 1991).

The above results clearly illustrate a significant strength of homotransfer measurements: the ability to detect band 3 self-association in situ and track its changes. On the other hand, the absolute sizes and fractional populations of a heterogeneous mix of oligomers would not be uniquely determined from the current homotransfer data. However, by adopting a simplified model of band 3 oligomerization, it was found that a fraction of large clusters is not required to interpret the homotransfer data. The anisotropy value for large clusters of band 3 was taken from the zinc-treated ghosts, which were verified to be rotationally immobilized by phosphorescence anisotropy. The HPLC-purified aggregate species was not used, because of the possibility that the detergent-solubilized material may not accurately represent clusters inside the ghost membrane. The melittin-treated species was not used in this calculation because anisotropy data suggest that melittin intercalates into the clusters, thereby increasing the EMA-EMA distance for homotransfer (see Clague and Cherry, 1989, for a proposed mechanism of clustering). The EMA-EMA distances within an endogenous band 3 cluster would probably be more similar to those in the zinc-induced species. Importantly, it was verified that no irreversible aggregation or denaturation processes are occurring during the zinc treatment, suggesting that the system is minimally perturbed. Considering whether the three-species model could be an oversimplification, it is noted that an intermediate-sized cluster species might exhibit an intermediate level of homotransfer, with a greater fraction of EMA molecules on the border of the cluster. However, this does not affect the finding that dimeric and tetrameric species alone can explain the homotransfer data, without including any larger clusters. As more information becomes available, such as the distance between the two EMA molecules in a band 3 dimer, or more detailed time-resolved fluorescence anisotropy measurements (which should reveal a distribution of anisotropy decay rates), the distribution of oligomeric states could be more precisely determined. Reconstitution studies should be especially useful in determining the anisotropy of band 3 of known oligomeric state in lipid bilayers.

CONCLUSIONS

The current studies have clearly shown that resonance energy homotransfer is occurring in EMA-labeled band 3, that the efficiency of homotransfer increases with increasing size of band 3 multimers, and that this homotransfer effect can be utilized as an assay for the self-association state of band 3 under various experimental conditions. The basic approach taken would be applicable to examination of the effects of hemichrome binding (McPherson et al., 1992), cell aging (Corbett and Golan, 1993), and anesthetic treatment (Cobb et al., 1990) on band 3 self-assembly, to cite only a few relevant examples. The findings reported here indicate that band 3 is predominantly if not entirely dimeric and/or tetrameric in ghost membranes, and show that the oligomeric state is not changed significantly by trypsin treatment. These results are consistent with previous size-exclusion HPLC experiments revealing only a small aggregate fraction, and with ST-EPR and freeze-fracture EM results discussed earlier. Most importantly, these data argue against the phenomenological interpretation of optical rotational diffusion data in terms of a large population of highly clustered band 3. Instead, it is suggested that protein-protein interactions (e.g., with the membrane skeletal proteins) constrain the rotational diffusion of band 3 without significantly perturbing its association state.

The authors thank Drs. J. R. Casey and A. M. Taylor (University of Alberta), C. E. Cobb, and E. J. Hustedt (Vanderbilt) for reviewing the manuscript before submission, and Dr. B. W. Van der Meer (Western Kentucky University) for many helpful discussions. Fluorescence lifetime experiments were performed at the Laboratory for Fluorescence Dynamics (LFD) at the University of Illinois at Urbana-Champaign (UIUC).

The LFD is supported jointly by the Division of Research Resources of the National Institutes of Health (RRO3155-01) and UIUC. This work was supported by grants HL34737 and T32GM07347 from the National Institutes of Health and by a grant from the Arnold and Mabel Beckman Foundation.

REFERENCES

Bastiaens, P. I. H., A. van Hoek, J. A. E. Benen, J.-C. Brochon, and A. J. W. G. Visser. 1992. Conformational dynamics and intersubunit energy transfer in wild-type and mutant lipoamide dehydrogenase from *Azotobacter vinelandii*: a multidimensional time-resolved polarized fluorescence study. *Biophys. J.* 63:839–853.

Beechem, J. M., E. Gratton, M. Ameloot, J. R. Knutson, and L. R. Brand. 1991. The global analysis of fluorescence and anisotropy decay data: Second-generation theory and programs. *In* Topics in Fluorescence Spectroscopy, Vol. 2: Principles. J. R. Lakowicz, editor. Plenum Press, New York. 241–305.

Bennett, V., and P. J. Stenbuck. 1979. The membrane attachment protein for spectrin is associated with band 3 in human erythrocyte membranes. *Nature.* 280:468–473.

Benz, R., M. T. Tosteson, and D. Schubert. 1984. Formation and properties of tetramers of band 3 protein from human erythrocyte membranes in planar lipid bilayers. *Biochim. Biophys. Acta.* 775:347–355.

Bicknese, S., M. Rossi, B. Thevenin, S. B. Shohet, and A. S. Verkman. 1995. Anisotropy decay measurement of segmental dynamics of the anion binding domain in erythrocyte band 3. *Biochemistry.* 34: 10645–10651.

Blackman, S. M., C. E. Cobb, A. H. Beth, and D. W. Piston. 1996. The orientation of eosin-5-maleimide on human erythrocyte band 3 measured by fluorescence polarization microscopy. *Biophys. J.* 71:194–208.

Blackman, S. M., D. W. Piston, and A. H. Beth. 1998. Self-association of human erythrocyte band 3 in situ: a simple fluorescence assay based on resonance energy homotransfer. *Biophys. J.* 74:A393.

Blackman, S. M., B. W. Van der Meer, D. W. Piston, and A. H. Beth. 1997. Resonance energy homotransfer in eosin-labeled band 3 in erythrocyte membranes demonstrated by time-resolved fluorescence and confocal microscopy. *Biophys. J.* 72:A201.

Bojarski, C., and K. Sienicki. 1990. Energy transfer and migration in fluorescent solutions. *In* Photochemistry and Photophysics, Vol. I. J. F. Rabek, editor. CRC Press, Boca Raton, FL. 1–57.

Casey, J. R., D. M. Lieberman, and R. A. F. Reithmeier. 1989. Purification and characterization of band 3 protein. *Methods Enzymol.* 173:494–512.

Casey, J. R., and R. A. F. Reithmeier. 1991. Analysis of the oligomeric state of band 3, the anion transport protein of the human erythrocyte membrane, by size exclusion high performance liquid chromatography: oligomeric stability and origin of heterogeneity. *J. Biol. Chem.* 266: 15726–15737.

Che, A., and R. J. Cherry. 1995. Loss of rotational mobility of band 3 proteins in human erythrocyte membranes induced by antibodies to glycophorin A. *Biophys. J.* 68:1881–1887.

Che, A., I. E. G. Morrison, R. Pan, and R. J. Cherry. 1997. Restriction by ankyrin of band 3 rotational mobility in human erythrocyte membranes and reconstituted lipid vesicles. *Biochemistry.* 36:9588–9595.

Cherry, R. J., A. Bürkli, M. Busslinger, and G. Schneider. 1976. Rotational diffusion of band 3 proteins in the human erythrocyte membrane. *Nature.* 263:389–393.

Clague, M. J., and R. J. Cherry. 1989. A comparative study of band 3 aggregation in erythrocyte membranes by melittin and other cationic agents. *Biochim. Biophys. Acta.* 980:93–99.

Clague, M. J., J. P. Harrison, and R. J. Cherry. 1989. Cytoskeletal restraints of band 3 rotational mobility in human erythrocyte membranes. *Biochim. Biophys. Acta.* 981:43–50.

Cobb, C. E., and A. H. Beth. 1990. Identification of the eosinyl-5-maleimide reaction site on the human erythrocyte anion-exchange protein: overlap with the reaction sites of other chemical probes. *Biochemistry.* 29:8283–8290.

Cobb, C. E., S. Juliao, K. Balasubramanian, J. V. Staros, and A. H. Beth. 1990. Effects of diethyl ether on membrane lipid ordering and on rotational dynamics of the anion exchange protein in intact human erythrocytes: correlations with anion exchange function. *Biochemistry.* 29:10799–10806.

Corbett, J. D., and D. E. Golan. 1993. Band 3 and glycophorin are progressively aggregated in density-fractionated sickle and normal red blood cells. *J. Clin. Invest.* 91:208–217.

Cuppoletti, J., J. Goldinger, B. Kang, I. Jo, C. Berenski, and C. Y. Jung. 1985. Anion carrier in the human erythrocyte exists as a dimer. *J. Biol. Chem.* 260:15714–15717.

Demchenko, A. P. 1986. Ultraviolet Spectroscopy of Proteins. Springer-Verlag, Heidelberg. 186–191.

Dissing, S., A. J. Jesaitis, and P. A. G. Fortes. 1979. Fluorescence labeling of the human erythrocyte anion transport system: subunit structure studied with energy transfer. *Biochim. Biophys. Acta.* 553:66–83.

Fairbanks, G., T. L. Steck, and D. F. H. Wallach. 1971. Electrophoretic analysis of the major peptides of the human erythrocyte membrane. *Biochemistry.* 10:2606–2617.

Golan, D. E., J. D. Corbett, C. Korsgren, H. S. Thatte, S. Hayette, Y. Yawata, and C. M. Cohen. 1996. Control of band 3 lateral and rotational mobility by band 4.2 in intact erythrocyte: release of band 3 oligomers from low-affinity binding sites. *Biophys. J.* 70:1534–1542.

Hui, S. W., C. M. Stewart, and R. J. Cherry. 1990. Electron microscopic observation of the aggregation of membrane proteins in human erythrocyte by melittin. *Biochim. Biophys. Acta.* 1023:335–340.

Hustedt, E. J., and A. H. Beth. 1995. Analysis of saturation-transfer electron paramagnetic resonance spectra of a spin-labeled integral membrane protein, band 3, in terms of the uniaxial rotational diffusion model. *Biophys. J.* 69:1409–1423.

Hustedt, E. J., and A. H. Beth. 1996. The determination of the orientation of a band 3 affinity spin-label relative to the membrane normal axis of the human erythrocyte. *Biochemistry.* 35:6944–6954.

Jähnig, F. 1986. The shape of a membrane protein derived from rotational diffusion. *Eur. Biophys. J.* 14:63–64.

Jennings, M. L. 1984. Oligomeric structure and the anion transport function of human erythrocyte band 3 protein. *J. Membr. Biol.* 80:105–117.

Jennings, M. L., and J. S. Nicknish. 1985. Localization of a site of intermolecular cross-linking in human red blood cell band 3 protein. *J. Biol. Chem.* 260:5472–5479.

Karolin, J., M. Fa, M. Wilczynska, T. Ny, and L. B.-A. Johansson. 1998. Donor-donor energy migration for determining intramolecular distances in proteins. I. Application of a model to the latent plasminogen activator inhibitor-1 (PAI-1). *Biophys. J.* 74:11–21.

Kawski, A. 1983. Excitation energy transfer and its manifestation in isotropic media. *Photochem. Photobiol.* 38:487–508.

Laemmli, U. K. 1970. Cleavage of structural proteins during the assembly of the head of bacteriophage T4. *Nature.* 227:680–685.

Lakowicz, J. R. 1983. Principles of Fluorescence Spectroscopy. Plenum Press, New York.

Liu, S.-Q. J., and P. A. Knauf. 1993. Lys-430, site of irreversible inhibition of band 3 Cl^- flux by eosin-5-maleimide, is not at the transport site. *Am. J. Physiol.* 264 (*Cell Physiol.* 33):C1155–C1164.

Macara, I. G., and L. C. Cantley. 1981. Interactions between transport inhibitors at the anion binding sites of the band 3 dimer. *Biochemistry.* 20:5095–5105.

Macara, I. G., S. Kuo, and L. C. Cantley. 1983. Evidence that inhibitors of anion exchange induce a transmembrane conformational change in band 3. *J. Biol. Chem.* 258:1785–1792.

Matayoshi, E. D., and T. M. Jovin. 1991. Rotational diffusion of band 3 in erythrocyte membranes. 1. Comparison of ghosts and intact cells. *Biochemistry.* 30:3527–3538.

McPherson, R. A., W. H. Sawyer, and L. Tilley. 1992. Rotational diffusion of the erythrocyte integral membrane protein band 3: effect of hemichrome binding. *Biochemistry.* 31:512–518.

McPherson, R. A., W. H. Sawyer, and L. Tilley. 1993. Band 3 mobility in camelid elliptocytes: implications for erythrocyte shape. *Biochemistry.* 32:6696–6702.

Michaely, P., and V. Bennett. 1995. The ANK repeats of erythrocyte ankyrin form two distinct but cooperative binding sites for the erythrocyte anion exchanger. *J. Biol. Chem.* 270:22050–22057.

Mulzer, K., L. Kampmann, P. Petrasch, and D. Schubert. 1991. Complex associations between membrane proteins analyzed by analytical ultracentrifugation: studies on the erythrocyte membrane proteins band 3 and ankyrin. *Colloid Polym. Sci.* 260:60–64.

Nigg, E. A., and R. J. Cherry. 1979a. Dimeric association of band 3 in the erythrocyte membrane demonstrated by protein diffusion measurements. *Nature.* 277:493–494.

Nigg, E. A., and R. J. Cherry. 1979b. Influence of temperature and cholesterol on the rotational diffusion of band 3 in the human erythrocyte membrane. *Biochemistry.* 18:3457–3465.

Nigg, E. A., and R. J. Cherry. 1980. Anchorage of a band 3 population at the erythrocyte cytoplasmic membrane surface: protein rotational diffusion measurements. *Proc. Natl. Acad. Sci. USA.* 77:4702–4706.

Palek, J., and S. Lambert. 1990. Genetics of the red cell membrane skeleton. *Semin. Hematol.* 27:290–332.

Peters, L. L., R. A. Shivdasani, S.-C. Liu, M. Hanspal, K. M. John, J. M. Gonzalez, C. Brugnara, B. Gwynn, N. Mohandas, S. L. Alper, S. H. Orkin, and S. E. Lux. 1996. Anion exchanger 1 (band 3) is required to prevent erythrocyte membrane surface loss but not to form the membrane skeleton. *Cell.* 86:917–927.

Pinder, J. C., A. Pekrun, A. M. Maggs, A. P. R. Brain, and W. B. Gratzer. 1995. Association state of human red blood cell band 3 and its interaction with ankyrin. *Blood.* 85:2951–2961.

Rodgers, W., and M. Glaser. 1993. Distributions of proteins and lipids in the erythrocyte membrane. *Biochemistry.* 32:12591–12598.

Runnels, L. W., and S. Scarlata. 1995. Theory and application of fluorescence homotransfer to melittin oligomerization. *Biophys. J.* 69: 1569–1583.

Rybicki, A. C., R. S. Schwartz, E. J. Hustedt, and C. E. Cobb. 1996. Increased rotational mobility and extractability of band 3 from protein 4.2-deficient erythrocyte membranes: evidence of a role for protein 4.2 in strengthening the band 3-cytoskeleton linkage. *Blood.* 88:2745–2753.

Saffman, P. G., and M. Delbrück. 1975. Brownian motion in biological membranes. *Proc. Natl. Acad. Sci. USA.* 72:3111–3113.

Schuck, P., B. Legrum, H. Passow, and D. Schubert. 1995. The influence of two anion-transport inhibitors, 4,4′-diisothiocyanatodihydrostilbene-2,2′-disulfonate and 4,4′-dibenzoylstilbene-2,2′-disulfonate, on the self-association of erythrocyte band 3 protein. *Eur. J. Biochem.* 230: 806–812.

Scothorn, D. J., W. E. Wojcicki, E. J. Hustedt, A. H. Beth, and C. E. Cobb. 1996. Synthesis and characterization of a novel spin-labeled affinity probe of human erythrocyte band 3: characteristics of the stilbenedisulfonate binding site. *Biochemistry.* 35:6931–6943.

Shi, Y., B. S. Karon, H. Kutchai, and D. D. Thomas. 1996. Phospholamban-dependent effects of $C_{12}E_8$ on calcium transport and molecular dynamics in cardiac sarcoplasmic reticulum. *Biochemistry.* 35: 13393–13399.

Southgate, C. D., A. H. Chishti, B. Mitchell, S. J. Yi, and J. Palek 1996. Targeted disruption of the murine erythroid band 3 gene results in spherocytosis and severe haemolytic anaemia despite a normal membrane skeleton. *Nature Genet.* 14:227–230.

Staros, J. V., and B. P. Kakkad. 1983. Cross-linking and chymotryptic digestion of the extracytoplasmic domain of the anion exchange channel in intact human erythrocytes. *J. Membr. Biol.* 74:247–254.

Steck, T. L. 1972. Cross-linking the major proteins of the isolated erythrocyte membrane. *J. Mol. Biol.* 66:295–305.

Tanaka, F., and N. Mataga. 1979. Theory of time-dependent photoselection in interacting fixed media. *Photochem. Photobiol.* 29: 1091–1097.

Thevenin, B. J.-M., and P. S. Low. 1990. Kinetics and regulation of the ankyrin-band 3 interaction of the human red blood cell membrane. *J. Biol. Chem.* 265:16166–16172.

Tsuji, A., K. Kawasaki, S. Ohnishi, H. Merkle, and A. Kusumi. 1988. Regulation of band 3 mobilities in erythrocyte ghost membranes by protein association and cytoskeletal meshwork. *Biochemistry.* 27: 7447–7452.

Turrini, F., P. Arese, J. Yuan, and P. S. Low. 1991. Clustering of integral membrane proteins of the human erythrocyte membrane stimulates autologous IgG binding, complement deposition, and phagocytosis. *J. Biol. Chem.* 266:23611–23617.

Van der Meer, B. W. 1993. Fluidity, dynamics, and order. *In* Biomembranes: Physical Aspects. M. Shinitzky, editor. VCH Publishers, New York. 98–158.

Van der Meer, B. W., G. Coker, III, and S.-Y. S. Chen. 1994. Resonance Energy Transfer: Theory and Data. VCH Publishers, New York.

Wang, D. N. 1994. Band 3 protein: structure, flexibility and function. *FEBS Lett.* 346:26–31.

Wang, D. N., W. Kühlbrandt, V. E. Sarabia, and R. A. F. Reithmeier. 1993. Two-dimensional structure of the membrane domain of human band 3, the anion transport protein of the erythrocyte membrane. *EMBO J.* 12:2233–2239.

Wang, D. N., V. E. Sarabia, R. A. F. Reithmeier, and W. Kühlbrandt. 1994. Three-dimensional map of the dimeric membrane domain of the human erythrocyte anion exchanger, band 3. *EMBO J.* 13:3230–3235.

Weber, G. 1960. Fluorescence-polarization spectrum and electronic energy transfer in tyrosine, tryptophan and related compounds. *Biochem. J.* 75:335–345.

Weinstein, R. S., J. K. Khodadad, and T. L. Steck. 1980. The band 3 protein intramembrane particle of the human red blood cell. *In* Membrane Transport in Erythrocytes. U. V. Llassen, H. H. Ussing, and J. O. Wieth, editors. Munksgaard, Copenhagen. 35–50.

Wolber, P. K., and B. S. Hudson. 1979. An analytic solution to the Förster energy transfer problem in two dimensions. *Biophys. J.* 28:197–210.

Wyatt, K., and R. J. Cherry. 1992. Both ankyrin and band 4.1 are required to restrict the rotational mobility of band 3 in the human erythrocyte membrane. *Biochim. Biophys. Acta.* 1103:327–330.

Yi, S. J., S.-C. Liu, L. H. Derick, J. Murray, J. E. Barker, M. R. Cho, J. Palek, and D. E. Golan. 1997. Red cell membranes of ankyrin-deficient *nb/nb* mice lack band 3 tetramers but contain normal membrane skeletons. *Biochemistry.* 36:9596–9604.

Zidovetzki, R., D. A. Johnson, D. J. Arndt-Jovin, and T. M. Jovin. 1991. Rotational mobility of high-affinity epidermal growth factor receptors on the surface of living A431 cells. *Biochemistry.* 30:6162–6166.

Zimet, D. B., B. J.-M. Thevenin, S. B. Shohet, and J. R. Abney. 1995. Calculation of resonance energy transfer in crowded biological membranes. *Biophys. J.* 68:1592–1603.